Journal of Cluster Science (2021) 32:995–1002
https://doi.org/10.1007/s10876-020-01864-x

ORIGINAL PAPER

One Pot Synthesis of Gentamicin Conjugated Gold Nanoparticles as an Efficient Antibacterial Agent

Deepak Sharma[1] · Abhishek Chaudhary[1]

Received: 3 March 2020 / Published online: 20 August 2020

Abstract

In the present study, we report a simple, robust, and eco-friendly one pot synthesis of gentamicin conjugated gold nanoparticles (G-GNPs), where gentamicin behaves dually as a reducing as well as a stabilizing agent. The resultant nanoparticles were characterized through different microscopic and spectroscopic techniques and found to be almost spherical in shape with hydrodynamic diameter of $\sim$ 15 nm along with excellent stability. The antibacterial potential was evaluated by well diffusion assay and showed that G-GNPs effectively inhibit the growth of gram-positive and gram-negative bacteria viz. *Escherichia coli* DH5α, *Escherichia coli* ATCC 25922 and *Staphylococcus aureus* MTCC 3160 ($p < 0.05$). Results also revealed that G-GNPs exhibit excellent antibacterial activity as compared with pure gentamicin, interestingly G-GNPs also showed excellent activity against gentamicin resistant *Escherichia fergusonii* ATCC 35469. A sustained release of gentamicin molecules from nanoparticles was observed. Furthermore, when we tested the effect of G-GNPs on mouse myoblast C2C12 cell line, G-GNPs exhibited minimal cytotoxicity. Consequently, the developed G-GNPs can be considered as safe based on minimal cytotoxicity of G-GNPs, and hold a great potential against gram-positive, gram-negative and drug resistance bacteria.

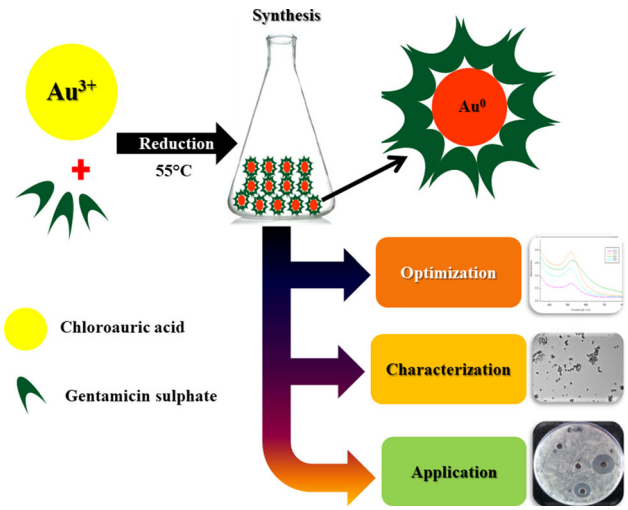

Keywords Gentamicin · Gold nanoparticles · Antibacterial effect · Drug release · Cytotoxicity

Introduction

Antibiotic resistance in pathogenic microorganisms is one of the potential threats to modern medicine that must be addressed to benefit mankind globally. Advance resistance

Electronic supplementary material The online version of this article (https://doi.org/10.1007/s10876-020-01864-x) contains supplementary material, which is available to authorized users.

✉ Abhishek Chaudhary
abhishekcbt@gmail.com; abhishek.chaudhary@juit.ac.in

[1] Department of Biotechnology and Bioinformatics, Jaypee University of Information Technology, Solan, Waknaghat, Himachal Pradesh 173234, India

mechanisms such as enzymatic modifications, decreased cell permeability, target protection, target overproduction, altered target site/enzyme, and increased efflux due to over-expression of efflux pumps, etc. are coming out and spreading extensively [1, 2]. Due to the antimicrobial resistance the treatable microbial infections such as tuberculosis, pneumonia, food-borne diseases, etc. are becoming difficult or sometimes impossible to cure [3]. The Centres for Disease Control and Prevention (CDC) estimates the mortality of 23,000 people per annum in the United States only due to antibiotic-resistant organisms. Moreover, antibiotic resistance is estimated to cause around 300 million premature deaths by 2050, with a loss of up to $100 trillion to the global economy [4]. Despite above mentioned concern, antibiotics are still a big weapon against bacterial infections. Gentamicin is such an antibiotic used extensively for treating variety of microbial infections because of its low cost and easy availability but large number of bacterial species had developed resistance against gentamicin through a variety of intrinsic and acquired mechanisms. *Escherichia fergusonii* ATCC 35469, a gentamicin resistance pathogen belongs to the genus *Escherichia* and family *Enterobacteriaceae* having 64% analogy to *Escherichia coli* that can cause diseases in animals and humans [5, 6]. A propitious way to combat gram-positive, gram-negative and drug resistance microbe is to use nanodrug or nanotherapeutics. In comparison to free drug molecule, nanodrug system can enhance the pharmacokinetics/pharmacodynamics, physiochemical properties, efficacy, and safety of drug molecule [7]. Generally, multiple steps are involved in the development of drug conjugated nanoparticles including nanoparticles synthesis, surface functionalization and loading of drug molecules [8, 9]. Moreover, hazardous chemicals are used in most of the steps which can cause undesirable results. In the present work, we have developed one pot synthesis method of gentamicin conjugated gold nanoparticles. The advantage of our approach is that it is one pot synthesis process and does not require any functionalization agent and harmful chemicals. The antibacterial property of gentamicin conjugated gold nanoparticles was determined against gram-positive, gram-negative and gentamicin resistance bacteria. Drug release of gold drug conjugate system was also investigated. Further, cytotoxicity of G-GNPs was determined on immortal mouse myoblast C2C12 cell line.

Materials and Methods

Materials

Hydrogen tetrachloroaurate (III) trihydrate was purchased from the Alfa Aesar, London, United Kingdom. Gentamicin sulphate, sodium hydroxide (NaOH), sodium chloride (NaCl), potassium chloride (KCl), disodium hydrogen phosphate, potassium dihydrogen phosphate, potassium hydroxide (KOH), sodium dodecyl sulphate (SDS), dialysis membrane-70, MTT, Muller Hinton broth and Muller Hinton agar were purchased from the HiMedia Laboratories Private Limited, Mumbai, India. Thiobarbituric acid (TBA) was purchased from Loba-Chemie, India, while nitro blue tetrazolium chloride (NBT) was from S D Fine Chemical Limited, India. Bovine serum albumin (BSA) was purchased from Super Religare Laboratories (SRL), India. Dulbecco's phosphate-buffered saline (PBS), fetal bovine serum (FBS), trypsin-ethylenediaminetetraacetic acid (EDTA) solution and Dulbecco's modified eagle medium (DMEM) were purchased from Thermo fisher, India. Dimethyl sulfoxide (DMSO) and methanol were obtained from Merck India. Mili Q water (18.2 mΩ) used in the study was from the Merck Millipore assembly of the institution.

Bacterial Cultures, Cell line and Their Maintenance

Bacterial cultures *E. coli* DH5α, *E. coli* ATCC 25922, *E. fergusonii* ATCC 35469 and *S. aureus* MTCC 3160 were procured from Department of Biotechnology and Bioinformatics, Jaypee University of Information Technology, Solan, India. All the cultures were maintained in Luria broth and were stored by making Luria agar plates and slants. Mouse myoblast cell line C2C12 was procured from the National Centre for Cell Science, Pune, India. Cell line was maintained in DMEM medium as per instructions from National Centre for Cell Science, Pune, India.

Synthesis of G-GNPs

The synthesis of gentamicin conjugated gold nanoparticles (G-GNPs) was achieved by reacting gentamicin (0.1 mM) with gold chloride (2.5 mM) in 1:1 ratio (Fig. S1) under alkaline condition (pH-11). The reaction was carried out at 55 °C (Fig. S2) under mild stirring condition and resultant particles were stored at 4 °C. Formation and stability of G-GNPs were monitored through UV–vis spectrophotometer at different time interval. All the reagents used

were prepared fresh and were stabilized to room temperature prior use.

Characterizations of G-GNPs

The morphology of synthesized nanoparticles (G-GNPs) were observed through TECNAI 200 kV (Fei, Electron Optics) transmission electron microscope (TEM) (Model: FP 5022/22-Tecnai G2 20 S-TWIN) with 200 kV accelerating voltage. The hydrodynamic size and dispersity of resultant nanoparticles were monitored through dynamic light scattering (DLS) using zeta-sizer nano (Instrument model: Malvern Instrument equipped with single photon counting avalanche photodiode and illuminated through He–Ne laser). Absorbance spectra was recorded through Thermo Scientific ^{TM} Evolution 201 UV–vis spectrophotometer. Microplate Reader (Bio-Rad) was used to perform the cytotoxic assay, and Fluorescence microscope (Nikon Eclipse-80i, Japan) was used to capture fluorescence images of bacterial cell.

Antibacterial Activity of G-GNPs

The antibacterial potential of G-GNPs was checked against *E. coli* DH5α, *E. coli* ATCC 25922, *E. fergusonii* ATCC 35469 and *S. aureus* MTCC 3160 using agar well plate diffusion assay. In brief, the aforementioned bacterial cultures were grown overnight in the Mueller–Hinton broth tubes then 50 µl volume of overnight grown cultures was spread on the Mueller–Hinton agar plates. The wells were made with the help of sterilized gel puncture having internal diameter of 3 mm. 15 µl of G-GNPs, gentamicin (0.5 µg equivalent) and gentamicin 6.0 µg equivalent (as control) was added into the respective wells for each culture. The plates were incubated at 37 °C for 16–18 h. The experiment was performed in triplicates and the results obtained were analysed by measuring the zone of inhibition.

Determination of Minimum Inhibitory Concentration

The minimum inhibitory concentrations (MIC) of G-GNPs, gold chloride and gentamicin sulphate were determined according to the protocol by Clinical & Laboratory Standards Institute (CLSI) [10]. The culture of *E. coli* DH5α, *E. coli* ATCC 25922, *E. fergusonii* ATCC 35469 and *S. aureus* MTCC 3160 were grown overnight in Muller Hinton broth tubes. The overnight grown cultures were diluted to achieve 1.5×10^8 cells/ml as per CLSI guidelines. A sterile 96 well plate was inoculated with sterile Mueller–Hinton broth, gentamicin sulphate (0–200 µg/ml), gold chloride (0–250 µg/ml) and G-GNPs (0–0.46 nM) respectively. A 10 µl diluted culture of each microorganism was added to their respective wells aseptically. Thereafter, well plate was incubated at 37 °C for 24 h. After incubation optical density (O.D.) of plate was taken at 600 nm and MIC was determined as described by Ahangari et al. [9].

Oxidative Stress Determination

Reactive Oxygen Species (ROS)

Metallic nanoparticles are well documented to kill microorganisms through the generation of reactive oxygen species. The enhanced level of reactive oxygen species due to G-GNPs was estimated by nitro blue tetrazolium (NBT) test as described by Choi et al. [11] with some modification. Briefly, the process involves the addition of 150 µl of G-GNPs (2.3 nM) to 3 ml overnight grown cultures of *E. coli* DH5α, *E. coli* ATCC 25922, *E. fergusonii* ATCC 35469 and *S. aureus* MTCC 3160 aseptically. The reaction mixture was incubated at 37 °C for 6 h. After incubation, the reaction mixture was centrifuged at 10,000 rpm for 10 min. The obtained pellet was dissolved in 2% NBT followed by incubation for 1 h at room temperature under dark conditions. After incubation, the system was centrifuged at 10,000 rpm for 10 min. The obtained pellet was washed with sodium phosphate buffer (0.1 M) and again centrifuged at 10,000 rpm for 10 min. 500 µl of 2 M KOH was added to the obtained pellet to disrupt the cell membrane followed by the addition of same volume of 50% DMSO. The reaction system was incubated at room temperature for 10 min to allow the solubilization of formazan crystals followed by centrifugation at 10,000 rpm for 10 min. The supernatant was used to observe the O.D. at 620 nm. The culture without nanoparticles treatment was used as a control while Mueller–Hinton broth medium was used as blank.

Determination of Membrane Lipid Peroxidation

Membrane lipid peroxidation (LPP) by oxidative stress in microbial cells has been well studied. It is reported in the literature that cell membrane lipids are the most suitable substrates for oxidative attack. Thiobarbituric acid reactive substances (TBARS) assay is commonly used to detect lipid peroxidation in various systems [12]. Malondialdehyde (MDA) is a toxic product formed due to the enzymatic and oxygen radical-induced lipid peroxidation. In the TBARS assay, malondialdehyde forms a complex

with thiobarbituric acid (TBA), which can be detected and quantified by spectrophotometer at 535 nm. 3 mL overnight grown bacterial cultures of *E. coli* DH5α, *E. coli* ATCC 25922, *E. fergusonii* ATCC 35469 and *S. aureus* MTCC 3160 were treated with 150 µl G-GNPs (2.3 nM) and were incubated at 37 °C in an orbital shaker for 6 h. After 6 h incubation period the cultures were centrifuged at 10,000 rpm for 10 min. Each obtained pellet was dispersed in the 500 µl of 10% SDS followed by addition of 20% acetic acid to this suspension and incubated for 10 min at room temperature. A 250 µl of TBA solution (0.8% TBA in 2 M NaOH) was added to the above solution. The whole reaction mixture was incubated for a period of 1 h at 95 °C followed by cooling to 25 °C. The reaction mixture was centrifuged at 10,000 rpm for 10 min. The obtained supernatant was used to determine the level of lipid peroxidation by measuring absorbance at 532 nm. The culture system without any treatment was considered as a control while the Mueller–Hinton broth was used as blank.

Membrane Disruption Determination

Membrane disruption by G-GNPs was determined as described by Zhao et al. [13]. The bacterial cultures of *E. coli* DH5α, *E. coli* ATCC 25922, *E. fergusonii* ATCC 35469 and *S. aureus* MTCC 3160 were incubated with 150 µl of G-GNPs (2.3 nM) for 12 h. After incubation bacterial cells were centrifuged at 6000 rpm for 5 min followed by twice washing with phosphate buffer saline (PBS). Bacterial cultures were thereafter incubated with 100 µM propidium iodide for 30 min and centrifuged at 6000 rpm for 5 min followed by twice washing with PBS. Thereafter 10 µl of cell suspension in PBS was placed on clean glass slide and was covered with cover slip. Bacteria without any treatment were taken as control. Cells having red fluorescence were counted using Nikon fluorescence microscope as an average of three individual measurements.

Drug Release Analysis

The drug release profile of gentamicin from G-GNPs was carried out at 37 °C and at neutral pH 7.3 in phosphate buffer saline (PBS). 1 ml of colloidal G-GNPs was transferred to dialysis beg and then immersed in PBS buffer at 37 °C. The samples were collected at specific time intervals to analyse the release of drug. The released drug was quantified by fluorescence spectroscopy method as described by Perni et al. [14]. A 100 µl of each *o*-phthalaldehyde (0.8 mg/ml) and isopropanol was mixed with 100 µl of sample and was incubated at room temperature in dark conditions for duration of 30 min. The fluorescence of samples was analysed at excitation wavelength 340 nm and emission wavelength 450 nm and quantified using standard calibration plot. The experiment was performed in triplicates.

Cytotoxicity Analysis

The cytotoxic effect of G-GNPs was determined on C2C12 cell line using MTT assay as described by Bahuguna et al. [15]. Briefly, 1×10^4 cells per well in DMEM having 10% FBS concentration were seeded in the 96 well plate and were incubated at 37 °C in CO_2 incubator for 24 h. After 24 h culture media was replaced with fresh medium and cells were treated with 150 µl of G-GNPs (2.3 nM), PBS and DMEM. The cell plate was again incubated at 37 °C in CO_2 incubator for 24 h. Further, 10 µl of MTT reagent (5 mg/ml in PBS) was added to each well and the plate was again incubated at 37 °C for 3–4 h. After incubation, 50 µl of DMSO was added to each well to solubilize formazan crystals and the plate was incubated at 37 °C for 30 min. The intensity due to formazan crystals was quantified at 540 nm.

Statistical Analysis

The experiments were performed in triplicates (n = 3) along with controls and were statistically analysed using ANOVA and Tukey's multiple comparison test ($p < 0.05$) with IBM SPSS version 20 (SPSS Inc., Chicago, IL, USA).

Results

Synthesis and Characterizations

The findings of Newman et al. [16] and Junqi et al. [17] were employed for the synthesis of G-GNPs where electron rich amine and hydroxyl group of gentamicin works as reducing and stabilizing agent for Au^{3+} to Au^0 conversion. Progression of the reaction was monitored visually by observing change in colour of gold chloride solution from pale yellow to wine red in presence of gentamicin (Fig. 1a) and further confirmed by UV–Vis spectrophotometer. An absorption band pertaining to the surface plasmon resonance (SPR) of gold nanoparticles appeared at 520 nm on completion of the reaction (Fig. 1c) confirmed the synthesis of nanoparticles however, no absorption peak was observed in the spectra of bare gentamicin and gold chloride in the range of 400–800 nm. Reaction was completed within 200 min, after that no further change was recorded in the absorption band at 520 nm indicating the completion of the reaction (Fig. 1d). Transmission electron microscopy and dynamic light scattering results revealed that,

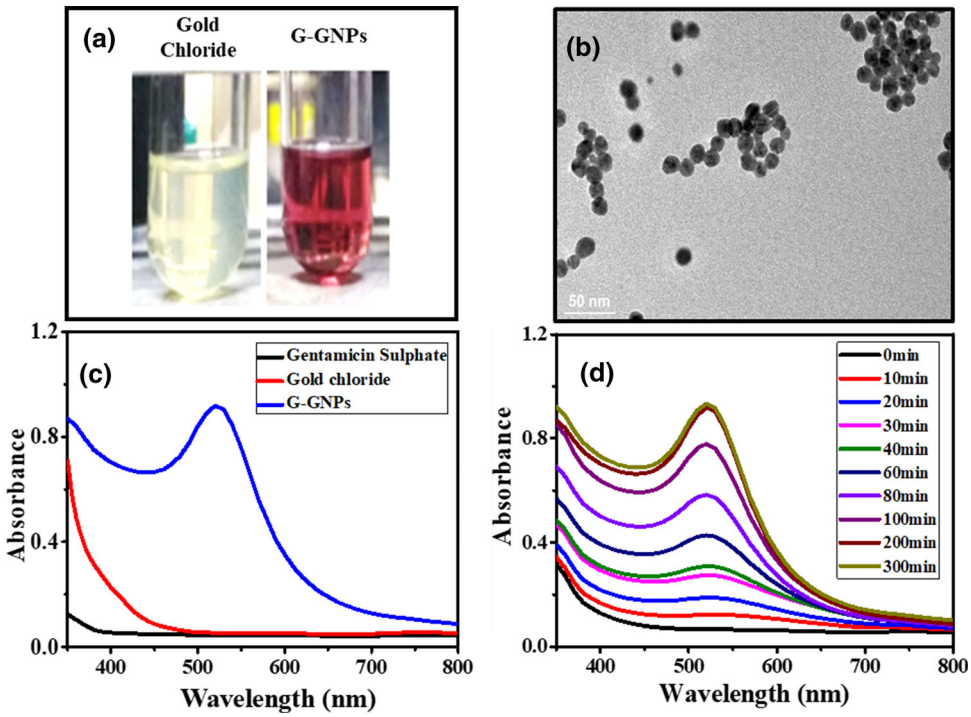

Fig. 1 **a** Photograph of gold chloride and G-GNPs respectively, **b** TEM image of G-GNPs **c** UV–Vis spectra of gold chloride (1.25 mM), gentamicin (0.05 mM) and G-GNPs (2.3 nM) and **d** Kinetics of G-GNPs formation monitored by the absorption spectra at different time periods

nanoparticles were spherical in shape and monodispersed with an average hydrodynamic diameter of 15 nm, which is in accordance with UV–Vis data (Fig. 1b and Fig. S3).The concentration of drug conjugated nanoparticles was 2.3 nM and was determined as described by Haiss et al. [18]. Synthesized particles were stable up to 1 month at 4 °C, as no significant change was observed in the absorption band till 1 month after that a second hump was appeared in the spectra indicating the aggregation of nanoparticles (Fig. S4).

Antibacterial Susceptibility Analysis and Determination of MIC Value

The antibacterial assay was performed by agar well diffusion method against *E. coli* DH5α, *E. coli* ATCC 25922, *E. fergusonii* ATCC 35469 and *S. aureus* MTCC 3160. Antibacterial susceptibility assay results showed that G-GNPs have synergistic inhibitory effect against all the tested microorganism. The zones of inhibition were observed between 9 and 15 mm for all the tested microorganisms with $p < 0.05$, whereas no visible zone of inhibition was observed with working concentration of gentamicin 0.5 µg equivalent. At higher gentamicin concentration of 6 µg equivalent, zone of inhibition was observed in all microorganisms except *E. fergusonii* ATCC 35469 (Fig. 2 and Table 1). Interestingly our synthesized G-GNPs were able to inhibit the growth of *E. fergusonii* ATCC 35469. The findings from current work revealed that the synthesized nanoparticles have good potential as

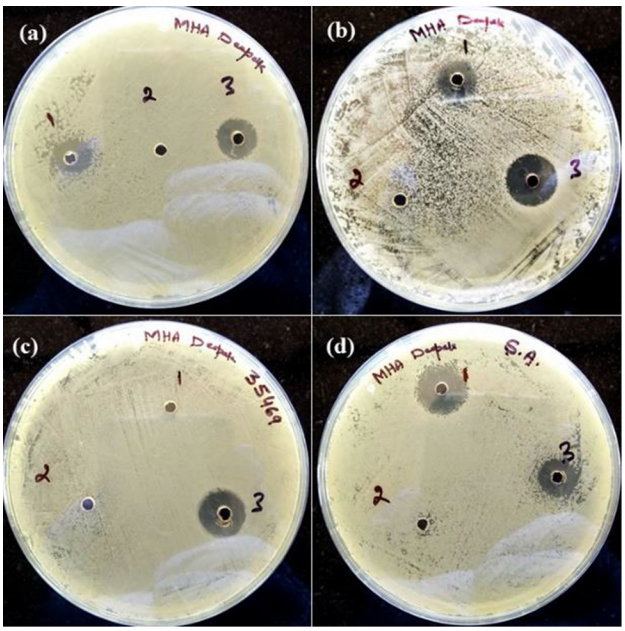

Fig. 2 Antibacterial activity of G-GNPs examined through well diffusion method. (well-1) 6 µg gentamicin sulphate equivalent, (well-2) Working conc. of gentamicin sulphate (0.5 µg equivalent), and (well-3) G-GNPs: **a** *E. coli* DH5α, **b** *E. coli* ATCC 25922, **c** *E. fergusonii* ATCC 35469, and **d** *S. aureus* MTCC 3160

antibacterial agent even in nanomolar concentration (Fig. 2 and Table 1). The effectiveness of G-GNPs against each bacterial culture was measured by estimating the MIC value. The MICs of G-GNPs against *E. coli* DH5α, *E. coli* ATCC 25922, *E. fergusonii* ATCC 35469 and *S. aureus*

Table 1 Calculation of inhibition zones (diameter in mm) caused by G-GNPs and gentamicin treatment

Well constituents	*E. coli* DH5α	*E. coli* ATCC 25922	*E. fergusonii* ATCC 35469	*S. aureus* MTCC 3160
Gentamicin sulphate (6 μg equivalent)	$9^{a,x}$	$10^{a,y}$	0	$14^{a,z}$
Working conc. of gentamicin sulphate (0.5 μg equivalent)	0	0	0	0
G-GNPs	$11^{b,x}$	$15^{b,z}$	$14^{a,y}$	$11^{b,x}$

[a, b] Means in the column with same superscript letter are not significantly different as measured by 2 sided Tukey's—post hoc range test between replications. [x–z] Means in the row with same superscript letter are not significantly different as measured by 2 sided Tukey's—post hoc range test between replications. However, there was no significant difference for all the culture against working conc. of gentamicin sulphate

Table 2 Minimum inhibitory concentrations of G-GNPs, gold chloride and gentamicin against both type of bacteria

Culture name	Gold chloride	Gentamicin	G-GNPs
E. coli DH5α	17 μg/ml^{a,x}	0.13 μg/ml^{a,y}	0.0046 nM^{a,z}
E. coli ATCC 25922	17 μg/ml^{a,x}	1.0 μg/ml^{b,y}	0.011 nM^{b,z}
E. coli ATCC 35469	68 μg/ml^{b,x}	>16.0 μg/ml^{c,y}	0.046 nM^{c,z}
S. aureus MTCC3160	68 μg/ml^{b,x}	1.0 μg/ml^{b,y}	0.0046 nM^{a,z}

[a–c] Means in the column with same superscript letter are not significantly different as measured by 2 sided Tukey's—post hoc range test between replications. [x–z] Means in the row with same superscript letter are not significantly different as measured by 2 sided Tukey's—post hoc range test between replications

MTCC 3160 were found to be 0.0046 nM, 0.01 nM, 0.046 nM and 0.0046 nM, respectively. The MICs of gentamicin and gold chloride was also determined (Table 2) and were many folds higher than the G-GNPs. The ionic form of gold (Au^{3+}) is toxic to bacteria as well as human blood keratinocytes and blood lymphocytes but reduced form (Au^{0}) is non-toxic. The possible mode of action of G-GNPs is in line with the literature, intracellular G-GNPs produce reactive oxygen species which is responsible for damage to ATP production, DNA replication and physical cell disruptions and finally bacterial cell death [19, 20].

Effect of G-GNPs on ROS and LPP

The enhancement in the level of reactive oxygen species after treatment with G-GNPs were evaluated against all the tested strain. The increments of 8.96%, 8.93%, 8.05% and 3.87% in the level of ROS was observed for *E. fergusonii* ATCC 35469, *S. aureus* MTCC 3160, *E. coli* ATCC 25922 and *E. coli* DH5α respectively (Fig. 3a). Induction of oxidative stress due to reactive oxygen species might be the possible mechanism of antibacterial activity [1, 21]. Furthermore, we have evaluated the effect of reactive oxygen species on the membrane lipid peroxidation. The increment of 9.33%, 8.21%, 6.35% and 4.76% in the lipid peroxidation level was found for *E. fergusonii* ATCC 35469, *S. aureus* MTCC 3160, *E. coli* ATCC 25922 and *E. coli* DH5α respectively (Fig. 3b). The enhanced level of ROS and membrane lipid peroxidation induce bacterial cell membrane disintegration, which is in accordance with the literature and supports the antibacterial activity of G-GNPs [12, 22].

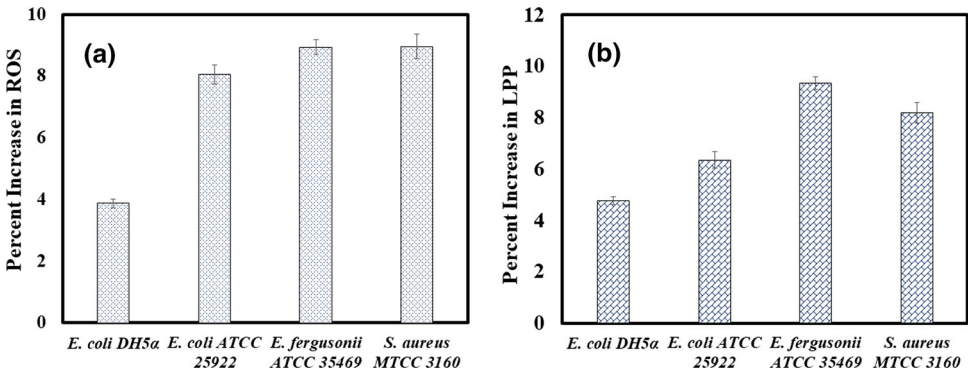

Fig. 3 Effect of G-GNPs treatment on the generation of **a** reactive oxygen species (ROS), and **b** lipid peroxidation (LPP)

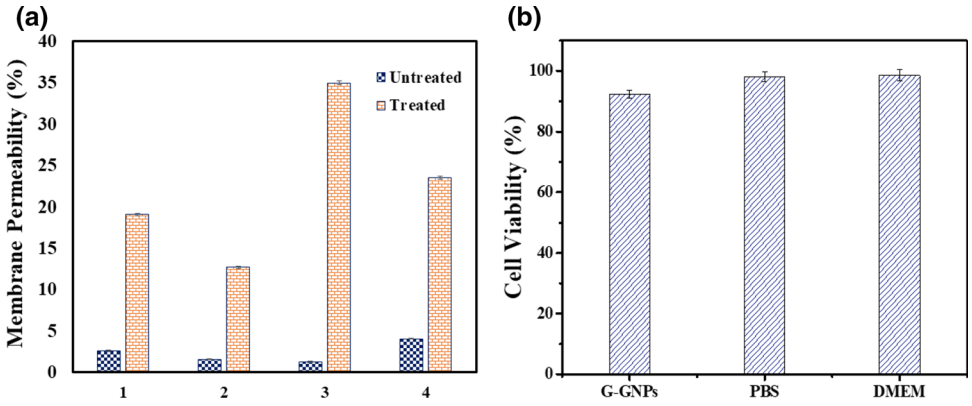

Fig. 4 **a** Effect of G-GNPs on bacterial cell membrane permeability: (1) *E. coli* DH5α, (2) *E. coli* ATCC 25922, (3) *E. fergusonii* ATCC 35469, and (4) *S. aureus* MTCC 3160, **b** cytotoxic effect of G-GNPs, PBS, and DMEM on the C2C12 cell line

Effect of G-GNPs on Bacterial Membrane Permeability

The damage to bacterial cell membrane was further investigated by staining of the cell with fluorescent dye propidium iodide (PI). Fluorescence microscopic image analysis confirmed the high killing of bacteria in the presence of G-GNPs as shown in Fig. 4a. The increment in the fluorescence intensity of bacterial cells incubated with G-GNPs was calculated using Image J software and found to be 35%, 23.54%, 19.1% and 12.7% for *E. fergusonii* ATCC 35469, *S. aureus* MTCC 3160, *E. coli* DH5α and *E. coli* ATCC 25922 respectively. The significant increase in the red fluorescence intensity of propidium iodide in G-GNPs treated bacteria was attributed by dead or compromised bacterial cells as compare to untreated bacteria [23]. The results clearly showed an increased membrane permeability of all the tested strain in response to treatment with G-GNPs, which confirmed the bactericidal effect of G-GNPs (Fig. S6).

Drug Release Analysis

The drug release behaviour of G-GNPs was investigated at physiological pH 7.3 for 72 h. The release profile showed that the drug release was maximum (37%) in the initial 8 h and then sustained release of drug was observed (Fig. S5). The possible mechanism behind the release of drug is stimulus dependent release; here pH act as stimuli to trigger the release of drug from G-GNPs. The shift in pH from alkali to physiological or acidic would increase the number of protons in the system, these protons break the electrostatic interaction between drug molecule and nanoparticles surface and hence accelerate the release of drug.

Cytotoxic Effect of G-GNPs on Cell line

The cytotoxic effect of G-GNPs was evaluated against mouse myoblast cell line C2C12. G-GNPs exhibit minimal cytotoxicity and 92.4% of cell viability even at higher concentration of G-GNPs (Fig. 4b). High cell viability of cell line in presence of G-GNPs advocates that the G-GNPs are biocompatible and can be used for nano drug development [24, 25].

Discussions

Although nanoscience has been increasingly used in the development of drug delivery systems, but multi step synthesis of drug conjugated nanoparticles limits its application as most of the steps are complicated and involve harsh chemical intermediate which can cause unwanted cell death [24]. In the present study a simple one pot synthesis method of gentamicin conjugated gold nanoparticles (G-GNPs) has been developed. The developed G-GNPs showed excellent antibacterial activity against gram-positive and gram-negative bacteria. The cell wall injuries due to physical interaction between G-GNPs and cell wall of gram-negative bacteria along with hydrophilic lipopolysaccharide layer facilitate the intake of G-GNPs into gram-negative bacteria while increase membrane permeability of gram-positive bacteria due to the leakage of Au^{3+} from nanoparticles enable the entry of G-GNPs into gram-positive bacteria [23, 26]. Intracellular G-GNPs leads to increase the formation of reactive oxygen species and lipid peroxidation that results the killing of bacterial cells. Furthermore, the computability of G-GNPs against mouse fibroblast cells (C2Cl2) was also assessed. C2C12 cell line exhibited more than 90% viability of cells at higher concentration of G-GNPs. The viability of C2Cl2 in presence of G-GNPs is due to the presence of cholesterol in the cell membrane, which help to stabilize the cell membrane and making them less sensitive to destruction by antibacterial G-GNPs [25]. Thus, from the current study it can be concluded that resultant nanoparticles (G-GNPs) hold the potential as therapeutic agents against gram-positive, gram-negative and as well as against gentamicin

resistant bacteria. The findings from this work will lead a step forward in the development of nano based antibacterial and other drugs.

Conclusions

An operational, environmental and time effective one pot synthesis strategy for the production of gentamicin conjugated gold nanoparticles (G-GNPs) has been developed. G-GNPs were effective against gram-negative, gram-positive, and drug resistant bacteria even in nanomolar concentration. The sustained release of gentamicin molecules from the gold nanoparticles with minimal cytotoxicity on C2C12 cell line advocates it as novel antibacterial agent.

Acknowledgements The work carried out in the present manuscript is supported by Jaypee University of Information Technology, Solan, India.

Compliance with Ethical Standards

Conflicts of Interest There are no conflicts between the authors to declare.

References

1. P. V. Baptistal, M. P. McCusker, A. Carvalho, D. A. Ferreira, N. M. Mohan, M. Martins, and A. R. Fernandes (2018). *Front. Microbiol.* **9**, 1441.
2. R. S. McInnes, G. E. McCallum, L. E. Lamberte, and W. van Schaik (2020). *Curr. Opin. Microbiol.* **53**, 35.
3. World Health Organisation. Antibiotic resistance. 2018.
4. J. M. Munita and C. A. Arias (2016). *Microbiol. Spectr.* **4**, 1.
5. J. J. Farmer, G. R. Fanning, B. R. Davis, C. M. O'hara, C. Riddle, F. W. Hickman-Brenner, M. A. Asbury, V. A. Lowery, and D. J. Brenner (1985). *J. Clin. Microbiol.* **21**, 77.
6. T. Adesina, O. Nwinyi, N. De, O. Akinnola, and E. Omonigbehin (2019). *Pathogens.* **8**, 164.
7. S. Onoue, S. Yamada, and H. K. Chan (2014). *Int. J. Nanomed.* **9**, 1025.
8. M. Salouti, Z. Heidari, A. Ahangari, and S. Zare (2016). *Drug Deliv.* **23**, 49.
9. A. Ahangari, M. Salouti, Z. Heidari, A. R. Kazemizadeh, and A. A. Safari (2013). *Drug Deliv.* **20**, 34.
10. Clinical and Laboratory Standards Institute (CLSI) (2012). CLSI Document M07-A9. Approved Standard. 9th Edition by Wayne, P. A.
11. H. Sim Choi, J. Woo Kim, Y. N. Cha, and C. Kim (2006). *J. Immunoassay Immunochem.* **27**, 31.
12. R. S. Thombre, V. Shinde, E. Thaiparambil, S. Zende, and S. Mehta (2016). *Front. Microbiol.* **7**, 1424.
13. Y. Zhao, Y. Tian, Y. Cui, W. Liu, W. Ma, and X. Jiang (2010). *J. Am. Chem. Soc.* **132**, 12349.
14. S. Perni and P. Prokopovich (2014). *RSC Advances.* **4**, 51904.
15. A. Bahuguna, I. Khan, V. K. Bajpai, and S. C. Kang (2017). *Bangladesh J. Pharmacol.* **12**, 8.
16. J. D. S. Newman and G. J. Blanchard (2006). *Langmuir.* **22**, 5882.
17. T. Junqi and M. Shiqing (2013). *Rare Metal Mat. Eng.* **42**, 2232.
18. W. Haiss, N. T. K. Thanh, J. Aveyard, and D. G. Fernig (2007). *Anal. Chem.* **79**, 4215.
19. P. Yang, P. Pageni, M. A. Rahman, M. Bam, T. Zhu, Y. P. Chen, M. Nagarkatti, A. W. Decho, and C. Tang (2019). *Adv. Healthc. Mater.* **8**, 1800854.
20. T. P. Shareena Dasari, Y. Zhang, and H. Yu (2015). *Biochem. Pharmacol.* **4**.
21. M. Y. Memar, R. Ghotaslou, M. Samiei, and K. Adibkia (2018). *Infect. Drug Resist.* **11**, 567.
22. V. Tiwari, N. Mishra, K. Gadani, P. S. Solanki, N. A. Shah, and M. Tiwari (2018). *Front. Microbiol.* **9**, 1218.
23. J. N. Payne, H. K. Waghwani, M. G. Connor, W. Hamilton, S. Tockstein, H. Moolani, F. Chavda, V. Badwaik, M. B. Lawrenz, and R. Dakshinamurthy (2016). *Front. Microbiol.* **7**, 607.
24. R. Shukla, V. Bansal, M. Chaudhary, A. Basu, R. R. Bhonde, and M. Sastry (2005). *Langmuir.* **21**, 10644.
25. X. Li, S. M. Robinson, A. Gupta, K. Saha, Z. Jiang, D. F. Moyano, A. S. M. A. Riley, and V. M. Rotello (2014). *ACS Nano.* **8**, 10682.
26. M. G. Ma in V. Basiuk and E. Basiuk (eds.), *Green Processes for Nanotechnology* (Springer, Cham, 2015), p. 119.